

# Unconditional Energy Stability Analysis of a Second Order Implicit–Explicit Local Discontinuous Galerkin Method for the Cahn–Hilliard Equation

Huailing Song<sup>1</sup> · Chi-Wang Shu<sup>2</sup>

Received: 28 February 2017 / Revised: 17 June 2017 / Accepted: 7 July 2017 /  
Published online: 14 July 2017  
© Springer Science+Business Media, LLC 2017

**Abstract** In this article, we present a second-order in time implicit–explicit (IMEX) local discontinuous Galerkin (LDG) method for computing the Cahn–Hilliard equation, which describes the phase separation phenomenon. It is well-known that the Cahn–Hilliard equation has a nonlinear stability property, i.e., the free-energy functional decreases with respect to time. The discretized Cahn–Hilliard system modeled by the IMEX LDG method can inherit the nonlinear stability of the continuous model. We apply a stabilization technique and prove unconditional energy stability of our scheme. Numerical experiments are performed to validate the analysis. Computational efficiency can be significantly enhanced by using this IMEX LDG method with a large time step.

**Keywords** Local discontinuous Galerkin method · Implicit–explicit · Second-order · Stability analysis · The Cahn–Hilliard equation

## 1 Introduction

The Cahn–Hilliard equation was originally introduced as a phenomenological model of phase separation in a binary alloy [6], which has been applied to a wide range of problems. It is given by

---

The first author was supported by NSFC (Grant No.11301167), Natural Science Foundation of Hunan Province, China (Grant No.14JJ3063) and by the China Scholarship Council (CSC). The second author was supported by DOE Grant DE-FG02-08ER25863 and NSF Grant DMS-1418750.

---

✉ Huailing Song  
shling@hnu.edu.cn

Chi-Wang Shu  
shu@dam.brown.edu

<sup>1</sup> College of Mathematics and Econometrics, Hunan University, Changsha 410082, People's Republic of China

<sup>2</sup> Division of Applied Mathematics, Brown University, Providence, RI 02912, USA

$$\begin{cases} \frac{\partial u}{\partial t} = \Delta \left( f(u) - \varepsilon^2 \Delta u \right), & (x, t) \in \Omega \times (0, T], \\ u|_{t=0} = u_0(x), & x \in \Omega. \end{cases} \tag{1}$$

Here,  $u_0(x)$  is a given function and  $\Omega \subset \mathbb{R}^d$  ( $d = 1, 2, 3$ ) is a bounded domain. We only focus on  $\mathbb{R}^2$  in this paper. Also, for easy presentation of the analysis, we assume a box geometry and a periodic boundary condition for  $u(\cdot, t)$ , however the method as well as the analysis can be generalized to Dirichlet boundary condition as well. The parameter  $\varepsilon$  is a positive constant and usually represents (the effect of) the interfacial energy in a phase separation phenomenon, which is small compared to the characteristic length of the laboratory scale [6]. The reaction term  $f(u) = F'(u)$ , with  $F(u) = \frac{1}{4}(u^2 - 1)^2$  being a given energy potential, drives the solution to the two pure states  $u = \pm 1$ .

Let the total free energy  $E(u)$  be defined by

$$E(u) = \int_{\Omega} \left( \frac{\varepsilon^2}{2} |\nabla u|^2 + F(u) \right) dx. \tag{2}$$

It is well known that the solution  $u(x, t)$  of the Cahn–Hilliard equation possesses the property that the total free energy  $E(u)$  decreases with respect to time, as the Cahn–Hilliard equation is the  $H^{-1}$ -gradient flow of the total free energy  $E(u)$  [6, 18]. We differentiate the energy  $E(u)$  and get

$$\begin{aligned} \frac{d}{dt} E(u) &= \int_{\Omega} \left( \varepsilon^2 |\nabla u| \cdot |\nabla u_t| + F'(u) u_t \right) dx \\ &= \int_{\Omega} \left( f(u) - \varepsilon^2 \Delta u \right) \cdot u_t dx \\ &= - \int_{\Omega} \left( \nabla (f(u) - \varepsilon^2 \Delta u) \right)^2 dx \leq 0. \end{aligned} \tag{3}$$

Therefore, the total energy is non-increasing in time and is a Lyapunov functional for the solution of the Cahn–Hilliard equation.

Designing numerical schemes that satisfy the energy-decay property at the discrete level has been extensively studied in the past. There have been many works [9, 11–13, 16, 21–23], and the references therein, on numerical analysis of the Cahn–Hilliard equation. Most of the analyses are based on finite element methods, finite difference methods or Fourier-spectral methods.

Finite element methods were first presented for the equation by Elliott et al. in [11, 12]. In [7], a conservative nonlinear finite difference scheme was proposed, which was unconditionally stable in the  $L^\infty$ -norm and conserved the total mass. However, the energy stability was not discussed. A linearized finite difference method was derived in [23]. Solvability and convergence were studied, but the stability was conditional. In [9], Furihata proposed a conservative difference method for solving the one-dimensional Cahn–Hilliard equation and proved the unconditional stability in the sense of energy decay.

Since the simulation of the Cahn–Hilliard equation needs very long time to reach the steady state, methods allowing large time steps are needed. In [18], a large time-stepping method was proposed for the Cahn–Hilliard equation. The time step can be increased by adding a linear term dependent on the unknown numerical solution. The same large time-stepping method was applied to the epitaxial growth models in [24]. In [20] and [27], adaptive time-stepping methods for the molecular beam epitaxy models and the Cahn–Hilliard equation were presented, respectively. The adaptive time step is selected based on the energy variation or the change of the roughness of the solution.

Later on, Shen and Yang [21] considered a few temporal discretization schemes for the Allen–Cahn and Cahn–Hilliard equations, such as the first-order semi-implicit and the second-order implicit schemes. They also showed energy stability under reasonable conditions and established error estimates for two fully discretized schemes with a spatial spectral–Galerkin approximation. Recently, Li and Qiao in [19] proposed a second-order semi-implicit Fourier spectral method for solving 2D Cahn–Hilliard equations. They introduced a new stabilization technique and proved the property of a decreasing total energy for the discrete scheme with a stabilization depending only on the initial value and the parameter  $\varepsilon$ . In this paper, we extend this new technique to the local discontinuous Galerkin method (LDG). This extension is non-trivial, as several discrete operators, such as an inverse Laplacian operator and a discrete Laplacian operator, as well as several properties, such as a broken version of the Brezis–Gallouet inequality, must be defined and analyzed for the LDG spatial discretization.

The LDG method was introduced by Cockburn and Shu in [8] as a generalization of the discontinuous Galerkin (DG) method proposed by Bassi and Rebay in [4]. The LDG method can be applied to PDEs containing higher order spatial derivatives, and the idea is to rewrite the equations with higher order derivatives as a first order system, then apply the DG method to the system with suitable numerical fluxes. For a detailed description about the LDG methods for high order time-dependent PDEs, we refer the readers to the review paper [25]. The LDG method possesses several properties which makes it very attractive for practical computations. For example, the method uses discontinuous-in-space approximations, is locally conservative, which is a crucial property in applications for porous media flows, transport phenomena, etc. From the computational point of view, since no inter-element continuity is imposed, the method can be defined on very general meshes including those with hanging nodes.

The LDG method for the spatial variables is usually combined with fully implicit time-discretization to avoid excessive restriction on the time steps. However, fully implicit schemes may be more difficult in efficient implementation, especially for the fully nonlinear Cahn–Hilliard equation. This is because such schemes require the solution of a coupled system of nonlinear equations per time step, making it computationally challenging to achieve it efficiently. Meanwhile, explicit methods have a strong restriction to the time steps. The small positive parameter  $\varepsilon$  and the nonlinear term of the Cahn–Hilliard equation make most of the finite difference methods to use time-step size of many orders of magnitude smaller than the spatial mesh size. Developing novel numerical techniques for this equation to overcome this difficulty has been extensively studied in the past, e.g., Eyre developed a convex-splitting method and proved that the method is unconditionally gradient stable [14, 15]. Guo and Xu [17] proposed efficient solvers of DG methods for the Cahn–Hilliard equation. Besides, it is known that implicit–explicit (IMEX) techniques have been introduced for time dependent partial-differential equations and can often play an important role in enhancing stability and efficiency [2, 3]. The IMEX schemes usually have large stability regions than other schemes over a wide parameter range. With this motivation, the implicit–explicit strategy is developed for the Cahn–Hilliard equation in this paper. In order to alleviate the stringent time-step restriction of explicit time discretization, we consider a class of implicit–explicit time discretization which treats the nonlinear terms explicitly and the linear terms implicitly. The spatial discretization is the standard local discontinuous Galerkin method. We perform an energy stability analysis on this fully discrete scheme.

The rest of the paper is organized as follows. In Sect. 2, we present some preliminaries and notations, which will be used in the whole paper. In this section, the IMEX LDG method is introduced, and the main theorem is given. In Sect. 3, we discuss two discrete operators and some auxiliary results. In Sect. 4, we prove the unconditional energy stability of the

IMEX LDG scheme. In Sect. 5, a few numerical experiments are carried out to confirm the theoretical results and to demonstrate the good performance of this method for the Cahn–Hilliard equation. Finally, some comments and conclusions are made in Sect. 6. A few technical proofs are given in the “Appendix”.

## 2 The IMEX LDG Methods for the Cahn–Hilliard Equation

### 2.1 Notations

In this section, we first introduce some notations, which will be used throughout the paper. We use  $H^m(\Omega)$  and  $\|\cdot\|_m$  to denote the standard Sobolev spaces and their norms, respectively. In particular, the norm and inner product of  $L^2(\Omega) = H^0(\Omega)$  are denoted by  $\|\cdot\|$  and  $(\cdot, \cdot)$  respectively.

Throughout the paper  $C$  will denote a generic positive constant, independent of the discretization parameters, whose value may change from line to line.

Let  $T_h = \{K\}$  be a quasi-uniform partition of the domain  $\Omega$  and set  $\partial T_h := \{\partial K : K \in T_h\}$ . For example, in the one-dimensional case,  $K$  is a subinterval; in the two-dimensional case,  $K$  is a shape-regular triangle for triangular meshes, or a shape-regular rectangle for Cartesian meshes. We will only consider up to two dimensions in this paper.

Associated with this mesh, we define the discontinuous finite element space

$$V_h = \{v \in L^2(\Omega) : v|_K \in P_k(K), \forall K \in T_h\},$$

$$\Phi_h = \left\{ \phi = (\phi_1, \dots, \phi_d)^T : \phi_i|_K \in P_k(K), i = 1, \dots, d, \forall K \in T_h \right\},$$

where  $P_k(K)$  denotes the space of polynomials in  $K$  of degree at most  $k \geq 0$ . Now we give the trace inequality with respect to the finite element space. For any function  $v \in V_h$ , there exists a positive inverse constant  $\mu > 0$  independent of  $v, h$  and  $K$  such that

$$\|v\|_{\partial K} \leq \sqrt{\mu h^{-1}} \|v\|_K. \tag{4}$$

Note that functions in  $V_h$  and  $\Phi_h$  are allowed to have discontinuities across element interfaces. At each element interface, for any function  $v$ , there are two traces along the right-hand and left-hand sides. In the one-dimension case, we define

$$v^\pm(x) = \lim_{\lambda \rightarrow 0} v(x \pm \lambda).$$

In the multi-dimension case, let  $e$  be an interior face shared by the elements  $K_1$  and  $K_2$ , and define the unit normal vectors  $\mathbf{n}_1$  and  $\mathbf{n}_2$  on  $e$  pointing exterior to  $K_1$  and  $K_2$ , respectively, i.e.  $\mathbf{n}_1 = -\mathbf{n}_2$ . We define the edge-jump and edge-average of  $v \in V_h$  by

$$[v] = v_1 \mathbf{n}_1 + v_2 \mathbf{n}_2, \quad \{v\} = \frac{1}{2}(v_1 + v_2),$$

where  $v_i = v|_{\partial K_i}$ . Similarly, for a vector-valued function  $\mathbf{w} \in \Phi_h$ , with an analogous definition of  $v_i, i = 1, 2$ ,

$$[\mathbf{w}] = \mathbf{w}_1 \cdot \mathbf{n}_1 + \mathbf{w}_2 \cdot \mathbf{n}_2, \quad \{\mathbf{w}\} = \frac{1}{2}(\mathbf{w}_1 + \mathbf{w}_2).$$

Let  $e_0$  be a fixed nonzero vector, we define

$$v^\pm = \{v\} \pm \gamma \cdot [v],$$

where  $\gamma$  is chosen by  $\gamma \cdot \mathbf{n} = \frac{1}{2} \text{sign}(e_0 \cdot \mathbf{n})$ .

### 2.2 The Implicit–Explicit LDG Methods

We start with the Cahn–Hilliard equation, and rewrite (1) as a first order system,

$$\begin{cases} u_t = \nabla \cdot (\mathbf{s}_1 - \mathbf{s}_2), \\ \mathbf{s}_1 = \nabla r, \\ \mathbf{s}_2 = \nabla p, \\ p = \varepsilon^2 \nabla \cdot \mathbf{w}, \\ \mathbf{w} = \nabla u, \\ r = f(u) \end{cases} \tag{5}$$

where  $u, \mathbf{s}_1, \mathbf{s}_2, p, \mathbf{w}, r$  are the auxiliary functions on  $\Omega$ .

We now consider the following second order in time implicit–explicit scheme,

$$\begin{cases} \frac{3u^{n+1} - 4u^n + u^{n-1}}{2\Delta t} + A\Delta t (u^{n+1} - u^n) = \nabla \cdot (\mathbf{s}_1^n - \mathbf{s}_2^{n+1}), \\ \mathbf{s}_1^n = \nabla r^n, \\ \mathbf{s}_2^{n+1} = \nabla p^{n+1}, \\ p^{n+1} = \varepsilon^2 \nabla \cdot \mathbf{w}^{n+1}, \\ \mathbf{w}^{n+1} = \nabla u^{n+1}, \\ r^n = 2f(u^n) - f(u^{n-1}) \end{cases} \tag{6}$$

where  $\Delta t > 0$  denotes the time step, and  $A$  is a positive constant. The above scheme combines second-order backward differentiation for the time derivative term with a second order extrapolation for the nonlinear term. The stabilization term  $A\Delta t (u^{n+1} - u^n)$  is added to enhance stability. Unfortunately, the parameter  $A$  must be chosen large enough to ensure stability, according to the analysis below and numerical experiments in Sect. 5.

In order to define the implicit–explicit (IMEX) LDG method to the Eq. (6), we still use  $u^{n+1}, \mathbf{s}_1^n, \mathbf{s}_2^{n+1}, p^{n+1}, \mathbf{w}^{n+1}, r^n$  to denote the numerical solutions. The IMEX LDG scheme is defined by an approximation

$$(u^{n+1}, \mathbf{s}_2^{n+1}, p^{n+1}, \mathbf{w}^{n+1}) \in V_h \times \Phi_h \times V_h \times \Phi_h,$$

such that,  $\forall \rho, \mathbf{q}, \phi, \psi, \xi \in V_h \times \Phi_h \times V_h \times \Phi_h \times V_h$  on each  $K \in T_h$ ,

$$\begin{aligned} & \left( \frac{3u^{n+1} - 4u^n + u^{n-1}}{2\Delta t}, \rho \right)_K + \left( A\Delta t \cdot (u^{n+1} - u^n), \rho \right)_K \\ & = - \left( (\mathbf{s}_1^n - \mathbf{s}_2^{n+1}), \nabla \rho \right)_K + \langle \hat{\mathbf{s}}_1^n - \hat{\mathbf{s}}_2^{n+1} \rangle \cdot \mathbf{n}, \rho \rangle_{\partial K}, \end{aligned} \tag{7}$$

$$(\mathbf{s}_1^n, \mathbf{q}_1)_K = -(r^n, \nabla \cdot \mathbf{q}_1)_K + \langle \hat{r}^n, \mathbf{q}_1 \cdot \mathbf{n} \rangle_{\partial K}, \tag{8}$$

$$(\mathbf{s}_2^{n+1}, \mathbf{q}_2)_K = -(p^{n+1}, \nabla \cdot \mathbf{q}_2)_K + \langle \hat{p}^{n+1}, \mathbf{q}_2 \cdot \mathbf{n} \rangle_{\partial K}, \tag{9}$$

$$(p^{n+1}, \phi)_K = -\varepsilon^2 (\mathbf{w}^{n+1}, \nabla \phi)_K + \varepsilon^2 \langle \hat{\mathbf{w}}^{n+1} \cdot \mathbf{n}, \phi \rangle_{\partial K}, \tag{10}$$

$$(\mathbf{w}^{n+1}, \psi)_K = -(u^{n+1}, \nabla \psi)_K + \langle \hat{u}^{n+1}, \psi \cdot \mathbf{n} \rangle_{\partial K}, \tag{11}$$

$$(r^n, \xi)_K = \left( 2f(u^n) - f(u^{n-1}), \xi \right)_K. \tag{12}$$

The hat terms in the equations above at the cell boundary from integration by parts are the so-called “numerical fluxes”, which are functions defined on the edges and should be designed based on different guiding principles for different PDEs to ensure stability. The flux choices affect the stability and the accuracy of the method, as well as properties such as sparsity and symmetry of the stiffness matrix; cf. [1, 8]. As we shall see, different choices for the numerical fluxes will lead to different methods. In this paper, we choose the so-called alternating fluxes introduced in [8], i.e. the numerical fluxes  $(\hat{u}, \hat{\mathbf{w}})$  are defined on inter-element faces as

$$\begin{aligned} \hat{\mathbf{s}}_1^n &= \{\mathbf{s}_1^n\} - \gamma \cdot [\mathbf{s}_1^n], & \hat{r}^n &= \{r^n\} + \gamma \cdot [r^n] \\ \hat{\mathbf{s}}_2^{n+1} &= \{\mathbf{s}_2^{n+1}\} - \gamma \cdot [\mathbf{s}_2^{n+1}], & \hat{p}^{n+1} &= \{p^{n+1}\} + \gamma \cdot [p^{n+1}], \\ \hat{\mathbf{w}}^{n+1} &= \{\mathbf{w}^{n+1}\} - \gamma \cdot [\mathbf{w}^{n+1}], & \hat{u}^{n+1} &= \{u^{n+1}\} + \gamma \cdot [u^{n+1}]. \end{aligned}$$

By the definition of jump and average, we have

$$\begin{aligned} \hat{\mathbf{s}}_1^n &= \mathbf{s}_1^{n,-}, & \hat{\mathbf{s}}_2^{n+1} &= \mathbf{s}_2^{n+1,-}, & \hat{r}^n &= r^{n,+}, \\ \hat{p}^{n+1} &= p^{n+1,+}, & \hat{\mathbf{w}}^{n+1} &= \mathbf{w}^{n+1,-}, & \hat{u}^{n+1} &= u^{n+1,+}. \end{aligned}$$

We define  $H_{\partial K}(v, \mathbf{w}) = \langle \hat{v}, \mathbf{w} \cdot \mathbf{n} \rangle_{\partial K} + \langle v, \hat{\mathbf{w}} \cdot \mathbf{n} \rangle_{\partial K} - \langle v, \mathbf{w} \cdot \mathbf{n} \rangle_{\partial K}$  as the numerical entropy flux, and choose the same numerical fluxes  $(\hat{v}, \hat{\mathbf{w}})$  as the alternating fluxes

$$\hat{v} = v^+, \quad \hat{\mathbf{w}} = \mathbf{w}^-.$$

Note that we can also choose

$$\hat{v} = v^-, \quad \hat{\mathbf{w}} = \mathbf{w}^+.$$

Using the definition of the numerical fluxes, we get the following property of the numerical entropy flux  $H_{\partial K}(v, \mathbf{w})$ .

**Lemma 1** [10] *Suppose  $e$  is an inter-element face shared by the elements  $K_1$  and  $K_2$ ; then*

$$H_{\partial K_1 \cap e}(v, \mathbf{w}) + H_{\partial K_2 \cap e}(v, \mathbf{w}) = 0, \tag{13}$$

for any  $v \in V_h$  and  $\mathbf{w} \in \Phi_h$ . Moreover, we have

$$\sum_{K \in T_h} H_{\partial K}(v, \mathbf{w}) = 0. \tag{14}$$

### 2.3 The Main Theorem

Considering the above second order in time IMEX LDG method, if we choose a good stabilization term  $A$ , we can prove the unconditional energy stability for a modified energy functional. We shall first state the main theorem as follows.

**Theorem 1** *(Unconditional stability for the IMEX LDG method) Consider the IMEX LDG finite element method (7)–(12) with  $\varepsilon > 0$  and  $\Delta t > 0$ . Assume  $u_0 \in H^4(\Omega)$  with mean zero. Denote  $E_0 = E(u_0)$  as the initial energy. There exists a constant  $C > 0$  depending only on  $E_0$  and  $u_0$ , such that if*

$$A \geq C (1 + \varepsilon^{-36} |\log \varepsilon|^8), \tag{15}$$

then

$$\tilde{E}(u^{n+1}) \leq \tilde{E}(u^n), \quad \forall n \geq 1$$

where  $\tilde{E}(u^n)$  is defined for  $n \geq 1$  as a modified energy functional:

$$\tilde{E}(u^n) := E(u^n) + \frac{1}{4\Delta t} \|\sigma_h^n\|^2 + \frac{1}{2} \|u^n - u^{n-1}\|^2 \tag{16}$$

where  $\sigma_h^n$  will be defined later.

To obtain this main theorem, let us begin with the introduction of several operators and lemmas.

### 3 Operators and Auxiliary Results

In this section we introduce some operators and auxiliary results, such as the LDG discrete “inverse Laplacian” operator, the discrete Laplacian operator, and the broken version of the Brezis–Gallouet inequality. They will be used in the energy stability proof later.

#### 3.1 The LDG Discrete “inverse Laplacian” Operator and Its Properties

We would like to introduce the LDG discrete “inverse Laplacian” operator  $(-\Delta)^{-1}$  on each  $K \in T_h$ . Let  $v = (-\Delta)^{-1}u$ , then we have the second-order elliptic boundary value problem

$$\begin{cases} -\Delta v = u, & x \in \Omega, \\ \text{periodic boundary.} \end{cases} \tag{17}$$

To obtain the LDG discrete “inverse Laplacian” operator  $(-\Delta)^{-1}$  on each  $K \in T_h$ , we first derive the LDG finite element method for the problem (17). We start with rewriting the above problem as follows:

$$\begin{cases} \nabla v = \sigma, \\ -\nabla \cdot \sigma = u. \end{cases} \tag{18}$$

Using the same triangulation  $T_h$  of  $\Omega$  and the discontinuous finite element spaces  $V_h, \Phi_h$ , we consider the following weak form: find  $v_h \in V_h$  and  $\sigma_h \in \Phi_h$  such that  $\forall \tau, \eta \in \Phi_h \times V_h$  on each  $K \in T_h$ ,

$$(u, \eta)_K = (\sigma_h, \nabla \eta)_K - \langle \hat{\sigma}_h \cdot \mathbf{n}, \eta \rangle_{\partial K}, \tag{19}$$

$$(\sigma_h, \tau)_K = -(v_h, \nabla \cdot \tau)_K + \langle \hat{v}_h, \tau \cdot \mathbf{n} \rangle_{\partial K}. \tag{20}$$

where  $\hat{\sigma}_h = \sigma_h^-$ ,  $\hat{v}_h = v_h^+$ .

We need the important lemma in [26] (Lemma 3.1), which illustrates a relationship between the gradient and the element interface jump of the numerical solution with the numerical solution of the gradient.

**Lemma 2** [26] *Suppose  $(v_h, \sigma_h)$  is the solution of (20), then there exists a positive constant  $C_\mu$  independent of  $h$  but dependent on the inverse constant  $\mu$ , such that*

$$\|\nabla v_h\| + \sqrt{\mu h^{-1}} \| [v_h] \|_{\partial T_h} \leq C_\mu \|\sigma_h\|, \tag{21}$$

where  $\|\cdot\| = \left( \sum_K \|\cdot\|_K^2 \right)^{\frac{1}{2}}$ ,  $\|\cdot\|_{\partial T_h} = \left( \sum_{e \in \partial T_h} \|\cdot\|_e^2 \right)^{\frac{1}{2}}$ .

Using the above important relationship, we have the following proposition.

**Proposition 1** (The existence and uniqueness) Consider the LDG method defined by the weak form (19) and (20), with the numerical fluxes defined by  $\hat{\sigma}_h = \sigma_h^-$ ,  $\hat{v}_h = v_h^+$ . It defines a unique approximate solution  $v_h = (-\Delta)^{-1}u$  in  $V_h^0 = \{v \in V_h, \int_{\Omega} v dx = 0\}$ .

The proof of Proposition 1 is presented in ‘‘Appendix A’’.

If we let  $u = u^{n+1} - u^n \in V_h$  and  $u = u^n - u^{n-1} \in V_h$  in Eq. (19) respectively, we can have

$$\begin{cases} (u^{n+1} - u^n, \eta)_K = (\sigma_h^{n+1}, \nabla \eta)_K - \langle \hat{\sigma}_h^{n+1} \cdot \mathbf{n}, \eta \rangle_{\partial K}, \\ (\sigma_h^{n+1}, \tau)_K = -(v_h^{n+1}, \nabla \cdot \tau)_K + \langle \hat{v}_h^{n+1}, \tau \cdot \mathbf{n} \rangle_{\partial K}. \end{cases} \tag{22}$$

and

$$\begin{cases} (u^n - u^{n-1}, \eta)_K = (\sigma_h^n, \nabla \eta)_K - \langle \hat{\sigma}_h^n \cdot \mathbf{n}, \eta \rangle_{\partial K}, \\ (\sigma_h^n, \tau)_K = -(v_h^n, \nabla \cdot \tau)_K + \langle \hat{v}_h^n, \tau \cdot \mathbf{n} \rangle_{\partial K}. \end{cases} \tag{23}$$

Using the above LDG discrete ‘‘inverse Laplacian’’ operator  $(-\Delta)^{-1}$ , we should have  $v_h^{n+1} = (-\Delta)^{-1}(u^{n+1} - u^n)$  and  $v_h^n = (-\Delta)^{-1}(u^n - u^{n-1})$ . So we can obtain the following lemma.

**Lemma 3** Suppose  $(v_h^{n+1}, \sigma_h^{n+1})$  and  $(v_h^n, \sigma_h^n)$  are the solutions of (22) and (23) respectively, we have

$$\sum_K (u^{n+1} - u^n, v_h^{n+1})_K = \sum_K (\sigma_h^{n+1}, \sigma_h^{n+1})_K. \tag{24}$$

$$\sum_K (\delta^2 u^{n+1}, v_h^{n+1})_K = \sum_K (\sigma_h^{n+1}, \sigma_h^{n+1} - \sigma_h^n)_K. \tag{25}$$

where  $\delta^2 u^{n+1} = u^{n+1} - 2u^n + u^{n-1}$ .

For clarity, we leave the proof of this lemma to ‘‘Appendix B’’.

### 3.2 The LDG Discrete Laplacian Operator

For the second-order elliptic problem with a periodic boundary condition

$$-\Delta u = f, \quad \text{in } \Omega \tag{26}$$

where  $f$  is a given function in  $L^2(\Omega)$ , from the above LDG discrete ‘‘inverse Laplacian’’ operator, we can derive the LDG discrete Laplacian operator through its first order version

$$\begin{cases} \nabla u = \mathbf{z}, \\ -\nabla \cdot \mathbf{z} = f. \end{cases}$$

Multiplying the first and second equations by the test functions  $\tau$  and  $\eta$ , respectively, and integrating on a subset  $K$  of  $T_h$ , we define the LDG ‘‘discrete Laplacian’’  $\Delta_h$  as follows: given  $u_h \in V_h$ , find  $-\Delta_h u_h \in V_h$  such that

$$(\mathbf{z}_h, \tau)_K = -(u_h, \nabla \cdot \tau)_K + \langle \hat{u}_h, \tau \cdot \mathbf{n} \rangle_{\partial K}, \tag{27}$$

$$(-\Delta_h u_h, \eta)_K = (\mathbf{z}_h, \nabla \eta)_K - \langle \hat{\mathbf{z}}_h \cdot \mathbf{n}, \eta \rangle_{\partial K}, \tag{28}$$

where  $\hat{u}_h = u_h^+$ ,  $\hat{\mathbf{z}}_h = \mathbf{z}_h^-$ . The well-posedness of the operator can be obtained in  $V_h^0$ .

By the definition of the LDG discrete Laplacian operator, we can rewrite the Eqs. (10) and (11) as

$$(p^{n+1}, \phi) = -\varepsilon^2 (-\Delta_h u^{n+1}, \phi). \tag{29}$$



### 3.3 The Broken Version of the Brezis–Gallouet Inequality

The well known Brezis–Gallouet interpolation inequality is an inequality valid in two dimensions. It shows that a function of two variables which is sufficiently smooth has an explicit bound, which depends only logarithmically on the second derivatives (see [5]):

$$\|u\|_\infty \leq C \left( 1 + \|u\|_1 \sqrt{\log(1 + \|\Delta u\|)} \right)$$

where  $C$  depends only on the domain.

An alternative version of the above inequality is

$$\|u\|_\infty \leq C(1 + \|u\|_1) \sqrt{\log(1 + \|\Delta u\|)}. \tag{30}$$

We can get the following broken version of the Brezis–Gallouet inequality, which will be needed in the next section.

**Lemma 4** For any  $u_h \in V_h^0 := \{v \in V_h : (v, 1) = 0\}$ , we have

$$\|u_h\|_\infty \leq C(1 + \|\mathbf{z}_h\|) \sqrt{\log(1 + \|\Delta_h u_h\|)}, \tag{31}$$

where  $\mathbf{z}_h$  satisfies

$$(\mathbf{z}_h, \boldsymbol{\tau})_K = -(u_h, \nabla \cdot \boldsymbol{\tau})_K + \langle \hat{u}_h, \boldsymbol{\tau} \cdot \mathbf{n} \rangle_{\partial K}, \quad \forall \boldsymbol{\tau} \in \Phi_h.$$

*Proof* For  $\forall u_h \in V_h^0, \exists! \lambda \in V_h^0$ , s.t.  $\lambda = -\Delta_h u_h$ , i.e.

$$(-\Delta_h u_h, \eta) = (\lambda, \eta) = (\mathbf{z}_h, \nabla \eta)_K - \langle \hat{\mathbf{z}}_h \cdot \mathbf{n}, \eta \rangle_{\partial K}. \tag{32}$$

For  $\lambda \in V_h^0, \exists! \delta_h = (-\Delta)^{-1} \lambda$ , which satisfies (19) and (20), i.e.

$$\begin{aligned} (\lambda, \eta) &= (\sigma_h, \nabla \eta)_K - \langle \hat{\sigma}_h \cdot \mathbf{n}, \eta \rangle_{\partial K}, \\ (\sigma_h, \boldsymbol{\tau})_K &= -(\delta_h, \nabla \cdot \boldsymbol{\tau})_K + \langle \hat{\delta}_h, \boldsymbol{\tau} \cdot \mathbf{n} \rangle_{\partial K}. \end{aligned}$$

This implies that

$$\begin{aligned} (\mathbf{z}_h - \sigma_h, \nabla \eta)_K - \langle \hat{\mathbf{z}}_h - \hat{\sigma}_h \cdot \mathbf{n}, \eta \rangle_{\partial K} &= 0, \\ (\mathbf{z}_h - \sigma_h, \boldsymbol{\tau})_K &= -(u_h - \delta_h, \nabla \cdot \boldsymbol{\tau})_K + \langle \hat{u}_h - \hat{\delta}_h, \boldsymbol{\tau} \cdot \mathbf{n} \rangle_{\partial K}. \end{aligned}$$

Taking  $\eta = u_h - \delta_h, \boldsymbol{\tau} = \mathbf{z}_h - \sigma_h$ , summing up over  $K$  and using the same argument as in Proposition 1, we can get that  $u_h = \delta_h$  in  $V_h^0$ .

On the other hand, we define the following adjoint elliptic problem

$$\begin{cases} \sigma = \nabla \delta, \\ \lambda = -\nabla \cdot \sigma \end{cases}$$

which is assumed to have the elliptic regularity:

$$\|\sigma\|_{H^1(\Omega)} + \|\delta\|_{H^2(\Omega)} \leq C\|\lambda\|. \tag{33}$$

Obviously,  $(\delta_h, \sigma_h)$  is the elliptic projection of  $(\delta, \sigma)$ , and satisfies

$$\begin{cases} (\sigma, \nabla \eta)_K - \langle \hat{\sigma} \cdot \mathbf{n}, \eta \rangle_{\partial K} = (\sigma_h, \nabla \eta)_K - \langle \hat{\sigma}_h \cdot \mathbf{n}, \eta \rangle_{\partial K}, \\ (\sigma_h, \boldsymbol{\tau})_K = -(\delta_h, \nabla \cdot \boldsymbol{\tau})_K + \langle \hat{\delta}_h, \boldsymbol{\tau} \cdot \mathbf{n} \rangle_{\partial K}. \end{cases}$$

Using Lemma in [26] (Lemma 3.2), we have

$$\|\delta - \delta_h\| \leq Ch^2 \|\delta\|_2$$

which yields the result

$$\begin{aligned} \|u_h\|_\infty &= \|\delta_h\|_\infty \leq \|\delta - \delta_h\|_\infty + \|\delta\|_\infty \\ &\leq Ch^{-1}\|\delta - \delta_h\| + (1 + \|\delta\|_1)\sqrt{\log(1 + \|\delta\|_2)} \\ &\leq Ch\|\delta\|_2 + (1 + \|\delta - \delta_h\|_1 + \|\delta_h\|_1)\sqrt{\log(1 + \|\delta\|_2)} \\ &\leq C(h\|\delta\|_2 + \|\delta_h\|_1 + 1)\sqrt{\log(1 + \|\delta\|_2)} \\ &\leq C(h\|\lambda\| + \|\delta_h\|_1 + 1)\sqrt{\log(1 + \|\lambda\|)}, \end{aligned}$$

where the last inequality is due to the elliptic regularity, namely  $\|\delta\|_2 \leq C\|\lambda\|$ .

For the estimate of  $h\|\lambda\|$ , taking  $\eta = \lambda$  in (32) and using the inverse property, we can have

$$\|\lambda\|^2 \leq \left( \|\nabla\lambda\| + \sqrt{\mu h^{-1}}\|[\lambda]_{\partial T_h}\| \right) \|\mathbf{z}_h\| \leq Ch^{-1}\|\lambda\| \|\mathbf{z}_h\|.$$

Applying the above inequality and Lemma 2, we obtain

$$\begin{aligned} \|u_h\|_\infty &\leq C(1 + \|\mathbf{z}_h\| + \|u_h\|_1) \cdot \sqrt{\log(1 + \|\Delta_h u_h\|)} \\ &\leq C(1 + \|\mathbf{z}_h\|) \cdot \sqrt{\log(1 + \|\Delta_h u_h\|)}. \end{aligned}$$

□

### 4 The Proof of the Energy Stability

In this section, we will prove the unconditional energy stability for the fully discrete implicit–explicit LDG scheme.

**Lemma 5** Consider the IMEX LDG scheme (7)–(12) in Sect. 2, we have

$$\begin{aligned} E(u^{n+1}) - E(u^n) &+ \sqrt{2\varepsilon^2 \left( \frac{1}{\Delta t} + A\Delta t \right)} \cdot \|u^{n+1} - u^n\|^2 \\ &+ \frac{1}{4\Delta t} \left[ \|\sigma_h^{n+1}\|^2 - \|\sigma_h^n\|^2 \right] + \frac{1}{2} \cdot \left( \|u^{n+1} - u^n\|^2 - \|u^n - u^{n-1}\|^2 \right) \\ &\leq \left[ \frac{3}{2} (\|u^{n+1}\|_\infty^2 + \|u^n\|_\infty^2) + \frac{(3\|u^n\|_\infty^2 + 3\|u^{n-1}\|_\infty^2 + 1)^2}{2} \right] \cdot \|u^{n+1} - u^n\|^2. \end{aligned}$$

Clearly if

$$\sqrt{2\varepsilon^2 \left( \frac{1}{\Delta t} + A\Delta t \right)} \geq \frac{3}{2} (\|u^{n+1}\|_\infty^2 + \|u^n\|_\infty^2) + \frac{(3\|u^n\|_\infty^2 + 3\|u^{n-1}\|_\infty^2 + 1)^2}{2}, \tag{34}$$

then

$$\begin{aligned} E(u^{n+1}) &+ \frac{1}{4\Delta t} \|\sigma_h^{n+1}\|^2 + \frac{1}{2} \cdot \|u^{n+1} - u^n\|^2 \\ &\leq E(u^n) + \frac{1}{4\Delta t} \|\sigma_h^n\|^2 + \frac{1}{2} \cdot \|u^n - u^{n-1}\|^2. \end{aligned}$$

*Proof* We take the test functions in (7), (8), (9), (10) and (12) as

$$\begin{aligned} \rho &= v_h^{n+1} = (-\Delta)^{-1}(u^{n+1} - u^n), \quad \mathbf{q}_1 = \mathbf{q}_2 = \sigma_h^{n+1}, \\ \phi &= (u^{n+1} - u^n), \quad \xi = (u^{n+1} - u^n). \end{aligned} \tag{35}$$

Using the definition of the LDG discrete “inverse Laplacian” operator  $(-\Delta)^{-1}$  in (19) and (20), we have

$$\begin{aligned} & \left( \frac{3u^{n+1} - 4u^n + u^{n-1}}{2\Delta t}, v_h^{n+1} \right)_K + \left( A\Delta t \cdot (u^{n+1} - u^n), v_h^{n+1} \right)_K \\ &= -\left( \mathbf{s}_1^n - \mathbf{s}_2^{n+1}, \nabla v_h^{n+1} \right)_K + \langle \hat{\mathbf{s}}_1^n - \hat{\mathbf{s}}_2^{n+1} \rangle \cdot \mathbf{n}, v_h^{n+1} \rangle_{\partial K}, \end{aligned} \tag{36}$$

$$\left( \mathbf{s}_1^n, \sigma_h^{n+1} \right)_K = -\left( r^n, \nabla \cdot \sigma_h^{n+1} \right)_K + \langle \hat{r}^n, \sigma_h^{n+1} \rangle \cdot \mathbf{n} \rangle_{\partial K}, \tag{37}$$

$$\left( \mathbf{s}_2^{n+1}, \sigma_h^{n+1} \right)_K = -\left( p^{n+1}, \nabla \cdot \sigma_h^{n+1} \right)_K + \langle \hat{p}^{n+1}, \sigma_h^{n+1} \rangle \cdot \mathbf{n} \rangle_{\partial K}, \tag{38}$$

$$\begin{aligned} & (p^{n+1}, u^{n+1} - u^n)_K \\ &= -\varepsilon^2 (\mathbf{w}^{n+1}, \nabla(u^{n+1} - u^n))_K + \varepsilon^2 \langle \hat{\mathbf{w}}^{n+1} \rangle \cdot \mathbf{n}, u^{n+1} - u^n \rangle_{\partial K}, \end{aligned} \tag{39}$$

$$(r^n, u^{n+1} - u^n)_K = \left( 2f(u^n) - f(u^{n-1}), u^{n+1} - u^n \right)_K. \tag{40}$$

Now the terms on the right-hand side of Eqs. (36), (37), (38) can be bounded from Eqs. (19), (20). Taking  $\tau = \mathbf{s}_1^n - \mathbf{s}_2^{n+1}$  and  $\eta = r^n - p^{n+1}$ ,

$$\begin{aligned} & \left( \sigma_h^{n+1}, \mathbf{s}_1^n - \mathbf{s}_2^{n+1} \right)_K + \left( v_h^{n+1}, \nabla \cdot (\mathbf{s}_1^n - \mathbf{s}_2^{n+1}) \right)_K \\ & \quad - \langle \hat{v}_h^{n+1}, (\mathbf{s}_1^n - \mathbf{s}_2^{n+1}) \rangle \cdot \mathbf{n} \rangle_{\partial K} = 0, \end{aligned} \tag{41}$$

$$\begin{aligned} & \left( u^{n+1} - u^n, r^n - p^{n+1} \right)_K - \left( \sigma_h^{n+1}, \nabla(r^n - p^{n+1}) \right)_K \\ & \quad + \langle \hat{\sigma}_h^{n+1} \rangle \cdot \mathbf{n}, r^n - p^{n+1} \rangle_{\partial K} = 0. \end{aligned} \tag{42}$$

Subtracting (41) from (36), subtracting the sum of (38) and (42) from (37), and using integration by parts, we obtain

$$\begin{aligned} & \left( \frac{3u^{n+1} - 4u^n + u^{n-1}}{2\Delta t}, v_h^{n+1} \right)_K + \left( A\Delta t \cdot (u^{n+1} - u^n), v_h^{n+1} \right)_K \\ &= -\left( \sigma_h^{n+1}, \mathbf{s}_1^n - \mathbf{s}_2^{n+1} \right)_K + H_{\partial K} \left( v_h^{n+1}, (\mathbf{s}_1^n - \mathbf{s}_2^{n+1}) \right), \end{aligned} \tag{43}$$

$$\left( \mathbf{s}_1^n - \mathbf{s}_2^{n+1}, \sigma_h^{n+1} \right)_K = \left( u^{n+1} - u^n, r^n - p^{n+1} \right)_K + H_{\partial K} \left( r^n - p^{n+1}, \sigma_h^{n+1} \right). \tag{44}$$

For the Eq. (11), we have

$$(\mathbf{w}^{n+1}, \psi)_K = -(u^{n+1}, \nabla \psi)_K + \langle \hat{u}^{n+1}, \psi \rangle \cdot \mathbf{n} \rangle_{\partial K}. \tag{45}$$

At the same time, we have

$$(\mathbf{w}^n, \psi)_K = -(u^n, \nabla \psi)_K + \langle \hat{u}^n, \psi \rangle \cdot \mathbf{n} \rangle_{\partial K}. \tag{46}$$

Taking  $\psi = \mathbf{w}^{n+1}$ , then subtracting (46) from (45), we have

$$\begin{aligned} & (\mathbf{w}^{n+1} - \mathbf{w}^n, \mathbf{w}^{n+1}) = (u^n - u^{n+1}, \nabla \mathbf{w}^{n+1})_K + \langle \hat{u}^{n+1} - \hat{u}^n, \mathbf{w}^{n+1} \rangle \cdot \mathbf{n} \rangle_{\partial K} \\ &= \left( \nabla(u^{n+1} - u^n), \mathbf{w}^{n+1} \right)_K - \langle u^{n+1} - u^n, \mathbf{w}^{n+1} \rangle \cdot \mathbf{n} \rangle_{\partial K} \\ & \quad + \langle \hat{u}^{n+1} - \hat{u}^n, \mathbf{w}^{n+1} \rangle \cdot \mathbf{n} \rangle_{\partial K} \\ &= \left( \nabla(u^{n+1} - u^n), \mathbf{w}^{n+1} \right)_K + H_{\partial K} \left( (u^{n+1} - u^n), \mathbf{w}^{n+1} \right) \\ & \quad - \langle \hat{\mathbf{w}}^{n+1} \rangle \cdot \mathbf{n}, u^{n+1} - u^n \rangle_{\partial K}. \end{aligned} \tag{47}$$

Subtracting (44) from (43), then adding to it the sum of (39) and  $\varepsilon^2$  times the difference of (47) and (40), we have

$$\begin{aligned} & \frac{1}{2\Delta t} \left( 3u^{n+1} - 4u^n + u^{n-1}, v_h^{n+1} \right)_K + \left( A\Delta t \cdot (u^{n+1} - u^n), v_h^{n+1} \right)_K \\ & + \varepsilon^2 (\mathbf{w}^{n+1} - \mathbf{w}^n, \mathbf{w}^{n+1})_K + \left( 2f(u^n) - f(u^{n-1}), u^{n+1} - u^n \right)_K \\ & = H_{\partial K} \left( v_h^{n+1}, \mathbf{s}^{n+1} \right) - H_{\partial K} \left( r^n - p^{n+1}, \sigma_h^{n+1} \right) + \varepsilon^2 \cdot H_{\partial K} \left( (u^{n+1} - u^n), \mathbf{w}^{n+1} \right) \end{aligned}$$

Summing up over  $K$ , with the numerical fluxes at the domain boundary and Lemma 1, we obtain

$$\begin{aligned} & \sum_{K \in T_h} \left\{ H_{\partial K} \left( v_h^{n+1}, \mathbf{s}^{n+1} \right) - H_{\partial K} \left( r^{n+1} - p^{n+1}, \sigma_h^{n+1} \right) \right. \\ & \left. + \varepsilon^2 \cdot H_{\partial K} \left( (u^{n+1} - u^n), \mathbf{w}^{n+1} \right) \right\} = 0. \end{aligned}$$

Noticing  $3u^{n+1} - 4u^n + u^{n-1} = 2(u^{n+1} - u^n) + \delta^2 u^{n+1}$  and using Lemma 3,

$$\begin{aligned} & \left( \frac{1}{\Delta t} + A\Delta t \right) \|\sigma_h^{n+1}\|^2 + \frac{1}{4\Delta t} \|\sigma_h^{n+1} - \sigma_h^n\|^2 + \frac{1}{4\Delta t} \left[ \|\sigma_h^{n+1}\|^2 - \|\sigma_h^n\|^2 \right] \\ & + \frac{\varepsilon^2}{2} \left( \|\mathbf{w}^{n+1}\|^2 - \|\mathbf{w}^n\|^2 + \|\mathbf{w}^{n+1} - \mathbf{w}^n\|^2 \right) \\ & = - \sum_K \left( 2f(u^n) - f(u^{n-1}), u^{n+1} - u^n \right)_K \end{aligned} \tag{48}$$

where we have applied the simple identity  $a(a - b) = 1/2[a^2 - b^2 + (a - b)^2]$ .

For the last nonlinear term, note that

$$2f(u^n) - f(u^{n-1}) = f(u^n) + (f(u^n) - f(u^{n-1})),$$

and recalling  $f(u) = F'(u)$ ,  $F(u) = (u^2 - 1)^2/4$  and  $f'(u) = 3u^2 - 1$ ,

$$\begin{aligned} F(u^{n+1}) - F(u^n) &= f(u^n) \cdot (u^{n+1} - u^n) + \frac{1}{2} f'(u^n + \theta_1(u^{n+1} - u^n)) \cdot (u^{n+1} - u^n)^2 \\ &= f(u^n) \cdot (u^{n+1} - u^n) + \frac{3}{2} (u^n + \theta_1(u^{n+1} - u^n))^2 \cdot (u^{n+1} - u^n)^2 - \frac{1}{2} (u^{n+1} - u^n)^2 \end{aligned}$$

where  $0 < \theta_1 < 1$ .

Because of the convexity of the function  $x^2$ , we have

$$(u^n + \theta_1(u^{n+1} - u^n))^2 \leq (1 - \theta_1)(u^n)^2 + \theta_1(u^{n+1})^2.$$

Therefore

$$\begin{aligned} & f(u^n) \cdot (u^{n+1} - u^n) \\ &= F(u^{n+1}) - F(u^n) + \frac{1}{2} (u^{n+1} - u^n)^2 - \frac{3}{2} (u^n + \theta(u^{n+1} - u^n))^2 \cdot (u^{n+1} - u^n)^2 \\ &\geq F(u^{n+1}) - F(u^n) + \frac{1}{2} (u^{n+1} - u^n)^2 - \frac{3}{2} (\|u^{n+1}\|_\infty^2 + \|u^n\|_\infty^2) \cdot (u^{n+1} - u^n)^2. \end{aligned}$$

Similarly, we have

$$\begin{aligned} &(f(u^n) - f(u^{n-1})) \cdot (u^{n+1} - u^n) = f'(u^{n-1} + \theta_2(u^n - u^{n-1})) \\ &\quad \cdot (u^n - u^{n-1}) \cdot (u^{n+1} - u^n) \\ &\geq -(3\|u^n\|_\infty^2 + 3\|u^{n-1}\|_\infty^2 + 1) \cdot (u^n - u^{n-1}) \cdot (u^{n+1} - u^n). \end{aligned}$$

Collecting the estimates, we obtain

$$\begin{aligned} &\left(\frac{1}{\Delta t} + A\Delta t\right) \|\sigma_h^{n+1}\|^2 + \frac{1}{4\Delta t} \|\sigma_h^{n+1} - \sigma_h^n\|^2 + \frac{1}{4\Delta t} \left[\|\sigma_h^{n+1}\|^2 - \|\sigma_h^n\|^2\right] \\ &\quad + \frac{\varepsilon^2}{2} \left(\|\mathbf{w}^{n+1}\|^2 - \|\mathbf{w}^n\|^2 + \|\mathbf{w}^{n+1} - \mathbf{w}^n\|^2\right) \\ &\quad + \sum_K \left(F(u^{n+1}) - F(u^n), 1\right)_K + \frac{1}{2} \|u^{n+1} - u^n\|^2 \\ &\leq \frac{3}{2} \left(\|u^{n+1}\|_\infty^2 + \|u^n\|_\infty^2\right) \cdot \|u^{n+1} - u^n\|^2 \\ &\quad + (3\|u^n\|_\infty^2 + 3\|u^{n-1}\|_\infty^2 + 1) \cdot \|u^n - u^{n-1}\| \cdot \|u^{n+1} - u^n\|. \end{aligned}$$

Applying the definition of  $E(u)$ ,

$$\begin{aligned} &E(u^{n+1}) - E(u^n) + \frac{1}{4\Delta t} \left[\|\sigma_h^{n+1}\|^2 - \|\sigma_h^n\|^2\right] \\ &\quad + \left(\frac{1}{\Delta t} + A\Delta t\right) \|\sigma_h^{n+1}\|^2 + \frac{\varepsilon^2}{2} \|\mathbf{w}^{n+1} - \mathbf{w}^n\|^2 + \frac{1}{2} \|u^{n+1} - u^n\|^2 \\ &\leq \frac{3}{2} \left(\|u^{n+1}\|_\infty^2 + \|u^n\|_\infty^2\right) \cdot \|u^{n+1} - u^n\|^2 \\ &\quad + (3\|u^n\|_\infty^2 + 3\|u^{n-1}\|_\infty^2 + 1) \cdot \|u^n - u^{n-1}\| \cdot \|u^{n+1} - u^n\|. \end{aligned}$$

By using the inequality  $2ab \leq a^2 + b^2$ ,

$$\begin{aligned} &\left(\frac{1}{\Delta t} + A\Delta t\right) \|\sigma_h^{n+1}\|^2 + \frac{\varepsilon^2}{2} \|\mathbf{w}^{n+1} - \mathbf{w}^n\|^2 \\ &\geq \sqrt{2\varepsilon^2 \left(\frac{1}{\Delta t} + A\Delta t\right)} \sum_K \left(\sigma_h^{n+1}, \mathbf{w}^{n+1} - \mathbf{w}^n\right)_K. \end{aligned}$$

From the LDG discrete “inverse Laplacian” and Eqs. (45), (46),

$$\begin{aligned} &(\mathbf{w}^{n+1} - \mathbf{w}^n, \psi) + (u^{n+1} - u^n, \nabla \psi)_K - \langle \hat{u}^{n+1} - \hat{u}^n, \psi \cdot \mathbf{n} \rangle_{\partial K} = 0, \\ &(u^{n+1} - u^n, \eta)_K - (\sigma_h^{n+1}, \nabla \eta)_K + \langle \hat{\sigma}_h^{n+1} \cdot \mathbf{n}, \eta \rangle_{\partial K} = 0. \end{aligned}$$

Taking  $\psi = \sigma_h^{n+1}$  and  $\eta = u^{n+1} - u^n$ ,

$$\left(\mathbf{w}^{n+1} - \mathbf{w}^n, \sigma_h^{n+1}\right)_K = \left(u^{n+1} - u^n, u^{n+1} - u^n\right)_K + H_{\partial K} \left(u^{n+1} - u^n, \sigma_h^{n+1}\right).$$

So we have

$$\begin{aligned} &\left(\frac{1}{\Delta t} + A\Delta t\right) \|\sigma_h^{n+1}\|^2 + \frac{\varepsilon^2}{2} \|\mathbf{w}^{n+1} - \mathbf{w}^n\|^2 \\ &\geq \sqrt{2\varepsilon^2 \left(\frac{1}{\Delta t} + A\Delta t\right)} \sum_K \left(u^{n+1} - u^n, u^{n+1} - u^n\right)_K. \end{aligned}$$

On the other hand,

$$\begin{aligned} & (3\|u^n\|_\infty^2 + 3\|u^{n-1}\|_\infty^2 + 1) \cdot \|u^n - u^{n-1}\| \cdot \|u^{n+1} - u^n\| \\ & \leq \frac{1}{2} \cdot \|u^n - u^{n-1}\|^2 + \frac{(3\|u^n\|_\infty^2 + 3\|u^{n-1}\|_\infty^2 + 1)^2}{2} \cdot \|u^{n+1} - u^n\|^2. \end{aligned}$$

Now we have

$$\begin{aligned} & E(u^{n+1}) - E(u^n) + \sqrt{2\varepsilon^2 \left( \frac{1}{\Delta t} + A\Delta t \right)} \cdot \|u^{n+1} - u^n\|^2 \\ & + \frac{1}{4\Delta t} \left[ \|\sigma_h^{n+1}\|^2 - \|\sigma_h^n\|^2 \right] + \frac{1}{2} \cdot \left( \|u^{n+1} - u^n\|^2 - \|u^n - u^{n-1}\|^2 \right) \\ & \leq \left[ \frac{3}{2} \left( \|u^{n+1}\|_\infty^2 + \|u^n\|_\infty^2 \right) + \frac{(3\|u^n\|_\infty^2 + 3\|u^{n-1}\|_\infty^2 + 1)^2}{2} \right] \cdot \|u^{n+1} - u^n\|^2. \end{aligned}$$

□

We should prove that the energy stability condition (34) is satisfied. The first step is to estimate  $\|u^{n+1}\|_\infty$ , then we shall inductively prove that the condition (15) suffices.

### 4.1 Estimate for $\|u^{n+1}\|_\infty$

**Lemma 6** Suppose  $\tilde{E}(u^n) \leq M, \tilde{E}(u^{n-1}) \leq M$  for some  $M \geq 0$  dependent of  $E(u^0)$ , ( $n \geq 1$ ). Then

$$\begin{aligned} \|u^{n+1}\|^2 & \lesssim 1 + \varepsilon^{-2}, \\ \|\mathbf{w}^{n+1}\|^2 & \lesssim \varepsilon^{-2} + \varepsilon^{-4}, \\ \|\Delta_h u^{n+1}\|^2 & \lesssim \frac{1}{\varepsilon^2 \Delta t} + \frac{A\Delta t}{\varepsilon^2} + \varepsilon^{-4}, \\ \|u^{n+1}\|_\infty & \leq C\sqrt{\varepsilon^{-2} + \varepsilon^{-4}} \cdot \sqrt{\log \left( 1 + \left( \frac{1}{\varepsilon^2 \Delta t} + \frac{A\Delta t}{\varepsilon^2} + \varepsilon^{-4} \right)^{\frac{1}{2}} \right)} \end{aligned}$$

where  $C$  is independent of  $\Delta t$  and  $\mathbf{w}^{n+1}$  satisfies

$$(\mathbf{w}^{n+1}, \psi)_K = - (u^{n+1}, \nabla \cdot \psi)_K + \langle \hat{u}^{n+1}, \psi \cdot \mathbf{n} \rangle_{\partial K}, \quad \forall \psi \in \Phi_h.$$

*Proof* Since  $E(u^n) \leq \tilde{E}(u^n) \leq M$ , we have

$$E(u^n) = \frac{\varepsilon^2}{2} \sum_K \|\mathbf{w}^n\|^2 + \sum_K (F(u^n), 1) \leq M,$$

So that

$$\|\mathbf{w}^n\| \lesssim \varepsilon^{-1}, \quad \|u^n\| \lesssim 1.$$

Similarly

$$\|\mathbf{w}^{n-1}\| \lesssim \varepsilon^{-1}, \quad \|u^{n-1}\| \lesssim 1.$$

Taking the test functions in (7), (8), (9), (10) and (11) as

$$\rho = \varepsilon^2 u^{n+1}, \quad \mathbf{q}_1 = \mathbf{q}_2 = -\varepsilon^2 \mathbf{w}^{n+1}, \quad \phi = p^{n+1} - r^n, \quad \psi = \varepsilon^2 (\mathbf{s}_1^n - \mathbf{s}_2^{n+1})$$

we have

$$\begin{aligned}
 & \varepsilon^2 \left( \frac{3u^{n+1} - 4u^n + u^{n-1}}{2\Delta t}, u^{n+1} \right)_K + \varepsilon^2 \left( A\Delta t \cdot (u^{n+1} - u^n), u^{n+1} \right)_K \\
 & + \varepsilon^2 \left( \mathbf{s}_1^n - \mathbf{s}_2^{n+1}, \nabla u^{n+1} \right)_K - \varepsilon^2 \langle (\hat{\mathbf{s}}_1^{n+1} - \hat{\mathbf{s}}_2^{n+1}) \cdot \mathbf{n}, u^{n+1} \rangle_{\partial K} = 0, \\
 & - \varepsilon^2 \left( \mathbf{s}_1^n, \mathbf{w}^{n+1} \right)_K - \varepsilon^2 \left( r^n - p^{n+1}, \nabla \cdot \mathbf{w}^{n+1} \right)_K \\
 & + \varepsilon^2 \langle \hat{r}^n - \hat{p}^{n+1}, \mathbf{w}^{n+1} \cdot \mathbf{n} \rangle_{\partial K} = 0, \\
 & - \varepsilon^2 \left( \mathbf{s}_2^{n+1}, \mathbf{w}^{n+1} \right)_K - \varepsilon^2 \left( r^n - p^{n+1}, \nabla \cdot \mathbf{w}^{n+1} \right)_K \\
 & + \varepsilon^2 \langle \hat{r}^n - \hat{p}^{n+1}, \mathbf{w}^{n+1} \cdot \mathbf{n} \rangle_{\partial K} = 0, \\
 & \left( p^{n+1}, p^{n+1} - r^n \right)_K + \varepsilon^2 \left( \mathbf{w}^{n+1}, \nabla (p^{n+1} - r^n) \right)_K \\
 & - \varepsilon^2 \langle \hat{\mathbf{w}}^{n+1} \cdot \mathbf{n}, p^{n+1} - r^n \rangle_{\partial K} = 0, \\
 & \varepsilon^2 \left( \mathbf{w}^{n+1}, \mathbf{s}_1^n - \mathbf{s}_2^{n+1} \right)_K + \varepsilon^2 \left( u^{n+1}, \nabla \cdot (\mathbf{s}_1^n - \mathbf{s}_2^{n+1}) \right)_K \\
 & - \varepsilon^2 \langle \hat{u}^{n+1}, (\mathbf{s}_1^n - \mathbf{s}_2^{n+1}) \cdot \mathbf{n} \rangle_{\partial K} = 0.
 \end{aligned}$$

Adding the above equations and using Lemma 1,

$$\begin{aligned}
 & \varepsilon^2 \left( \frac{3}{2\Delta t} + A\Delta t \right) \cdot \left( u^{n+1} - u^n, u^{n+1} \right)_K \\
 & - \frac{\varepsilon^2}{2\Delta t} \cdot \left( u^n - u^{n-1}, u^{n+1} \right)_K + \left( p^{n+1}, p^{n+1} - r^n \right)_K = 0.
 \end{aligned}$$

Reorganizing the above equality,

$$\begin{aligned}
 & \varepsilon^2 \left( \frac{3}{2\Delta t} + A\Delta t \right) \cdot \left( u^{n+1} - u^n, u^{n+1} \right)_K - \frac{\varepsilon^2}{2\Delta t} \cdot \left( u^n - u^{n-1}, u^{n+1} - u^n \right)_K \\
 & + \frac{\varepsilon^2}{2\Delta t} \cdot \left( u^n - u^{n-1}, u^n \right)_K + \left( p^{n+1}, p^{n+1} \right)_K = \left( p^{n+1}, r^n \right)_K.
 \end{aligned}$$

Summing up over  $K$ , we obtain

$$\begin{aligned}
 & \frac{\varepsilon^2}{2} \left( \frac{3}{2\Delta t} + A\Delta t \right) \cdot \left( \|u^{n+1}\|^2 - \|u^n\|^2 \right) + \frac{\varepsilon^2}{4\Delta t} \cdot \left( \|u^n\|^2 - \|u^{n-1}\|^2 \right) + \|p^{n+1}\|^2 \\
 & + \frac{\varepsilon^2}{2} \left( \frac{3}{2\Delta t} + A\Delta t \right) \cdot \|u^{n+1} - u^n\|^2 - \frac{\varepsilon^2}{2\Delta t} \sum_K \left( u^n - u^{n-1}, u^{n+1} - u^n \right)_K \\
 & + \frac{\varepsilon^2}{4\Delta t} \cdot \|u^n - u^{n-1}\|^2 \\
 & = \sum_K \left( p^{n+1}, r^n \right)_K \leq \frac{1}{2} \left( \|p^{n+1}\|^2 + \|r^n\|^2 \right).
 \end{aligned}$$

Obviously,

$$\begin{aligned}
 & \frac{\varepsilon^2}{2} \left( \frac{3}{2\Delta t} + A\Delta t \right) \cdot \|u^{n+1} - u^n\|^2 - \frac{\varepsilon^2}{2\Delta t} \sum_K \left( u^n - u^{n-1}, u^{n+1} - u^n \right)_K \\
 & + \frac{\varepsilon^2}{4\Delta t} \cdot \|u^n - u^{n-1}\|^2 \geq 0.
 \end{aligned}$$

So we have,

$$\begin{aligned} \frac{\varepsilon^2}{2} \left( \frac{3}{2\Delta t} + A\Delta t \right) \|u^{n+1}\|^2 &\leq \frac{\varepsilon^2}{2} \left( \frac{1}{\Delta t} + A\Delta t \right) \|u^n\|^2 \\ &+ \frac{\varepsilon^2}{4\Delta t} \|u^{n-1}\|^2 + \frac{1}{2} \|2f(u^n) - f(u^{n-1})\|^2. \end{aligned}$$

We can get the result  $\|u^{n+1}\|^2 \lesssim 1 + \varepsilon^{-2}$  (independent of  $\Delta t$ ).

At the same time, we also have

$$\|p^{n+1}\|^2 \leq \varepsilon^2 \left( \frac{1}{\Delta t} + A\Delta t \right) \|u^n\|^2 + \frac{\varepsilon^2}{2\Delta t} \|u^{n-1}\|^2 + \|r^n\|^2. \tag{49}$$

For the estimation of  $\|\Delta_h u^{n+1}\|$ , taking  $\phi = -\Delta_h u^{n+1}$  in (29), we obtain

$$\|\Delta_h u^{n+1}\|^2 = \frac{1}{\varepsilon^2} (p^{n+1}, \Delta_h u^{n+1}) \leq \frac{1}{\varepsilon^2} \|p^{n+1}\| \cdot \|\Delta_h u^{n+1}\|.$$

Then

$$\begin{aligned} \|\Delta_h u^{n+1}\|^2 &\leq \frac{1}{\varepsilon^4} \|p^{n+1}\|^2 \\ &\lesssim \left( \frac{1}{\varepsilon^2 \Delta t} + \frac{A\Delta t}{\varepsilon^2} \right) \|u^n\|^2 + \frac{1}{2\Delta t \varepsilon^2} \|u^{n-1}\|^2 + \frac{1}{\varepsilon^4} \|2f(u^n) - f(u^{n-1})\|^2 \\ &\lesssim \frac{1}{\varepsilon^2 \Delta t} + \frac{A\Delta t}{\varepsilon^2} + \frac{1}{\varepsilon^4} (\|u^n\|^3 + \|u^n\| + \|u^{n-1}\|^3 + \|u^{n-1}\|) \\ &\lesssim \frac{1}{\varepsilon^2 \Delta t} + \frac{A\Delta t}{\varepsilon^2} + \frac{1}{\varepsilon^4}. \end{aligned}$$

Finally, for the estimation of  $\|w^{n+1}\|$ , using the Eq.(48) and the boundedness of  $\tilde{E}(u^n)$  and  $\|u^{n+1}\|, \|u^n\|, \|u^{n-1}\|$ ,

$$\begin{aligned} \|w^{n+1}\|^2 &\leq \|w^n\|^2 + \frac{1}{4\varepsilon^2 \Delta t} \|\sigma_h^n\|^2 + \varepsilon^{-2} [\|2f(u^n) - f(u^{n-1})\|^2 + \|u^{n+1} - u^n\|^2] \\ &\lesssim \varepsilon^{-2} + \varepsilon^{-4}. \end{aligned}$$

We can apply Lemma 4 to obtain

$$\|u^{n+1}\|_\infty \leq C \sqrt{\varepsilon^{-2} + \varepsilon^{-4}} \cdot \sqrt{\log \left( 1 + \left( \frac{1}{\varepsilon^2 \Delta t} + \frac{A\Delta t}{\varepsilon^2} + \varepsilon^{-4} \right)^{\frac{1}{2}} \right)}. \tag{50}$$

□

### 4.2 Estimate for the First Step $u^1$

In order to start the iteration, we should computer  $u^1$  according to the following first-order scheme

$$\begin{cases} \left( \frac{u^1 - u^0}{t_1}, \rho \right)_K + (s_1^0 - s_2^1, \nabla \rho)_K - \langle (s_1^0 - s_2^1) \cdot \mathbf{n}, \rho \rangle_{\partial K} = 0, \\ (s_1^0 - s_2^1, \mathbf{q}) + (r^0 - p^1, \nabla \cdot \mathbf{q}) - \langle \hat{r}^0 - \hat{p}^1, \mathbf{q} \cdot \mathbf{n} \rangle_{\partial K} = 0, \\ (p^1, \phi) + \varepsilon^2 (w^1, \nabla \phi) - \varepsilon^2 \langle \hat{w}^1 \cdot \mathbf{n}, \phi \rangle_{\partial K} = 0, \\ (w^1, \psi) + (u^1, \nabla \cdot \psi) - \langle \hat{u}^1, \psi \cdot \mathbf{n} \rangle_{\partial K} = 0, \\ (r^0, \xi) = (f(u^0), \xi). \end{cases} \tag{51}$$



So we now have the following lemma

**Lemma 7** Consider the above scheme (51), and assume  $u_0 \in H^4(\Omega)$  with mean zero,

$$\begin{aligned} \|u^1\|^2 &\leq \|u^0\|^2 + \frac{t_1}{\varepsilon^2} \|f(u^0)\|^2, \\ \|\Delta_h u^1\|^2 &\leq \frac{1}{\varepsilon^2 t_1} \|u^0\|^2 + \frac{1}{\varepsilon^4} \|f(u^0)\|^2, \\ \|\mathbf{w}^1\|^2 &\leq C(E(u^0), \|u^0\|_{H^4}) \frac{1}{\varepsilon^2}, \\ \|u^1\|_\infty &\leq C\sqrt{1 + \varepsilon^{-1}} \cdot \sqrt{\log\left(1 + \left(\frac{1}{\varepsilon^2 t_1} + \varepsilon^{-4}\right)^{\frac{1}{2}}\right)}, \end{aligned}$$

where  $C$  is independent of  $\Delta t$  and only depends on the initial value.

The proof of this lemma is very similar to Lemma 6. We skip the details at present, but for the completeness of this paper, we put the concise proof in ‘‘Appendix C’’.

### 4.3 Proof of Theorem 1

In this proof we shall denote by  $C$  a generic constant which depends only on  $u^0$ . The value of  $C$  may vary from line to line. Let

$$M = \max\{\tilde{E}(u^1), E(u^0)\}.$$

We shall inductively prove the result for every  $n \geq 1$ :

$$\tilde{E}(u^{n+1}) \leq M, \quad \tilde{E}(u^{n+1}) \leq \tilde{E}(u^n),$$

We first check the case  $n = 1$ . Applying Lemma 6, let  $n = 1$ , then

$$\|\mathbf{w}^2\|^2 \lesssim \varepsilon^{-2} + \varepsilon^{-4}.$$

By Lemmas 4 and 6, we obtain

$$\|u^2\|_\infty \leq C\sqrt{\varepsilon^{-2} + \varepsilon^{-4}} \cdot \sqrt{\log\left(1 + \left(\frac{1}{\varepsilon^2 \Delta t} + \frac{A\Delta t}{\varepsilon^2} + \varepsilon^{-4}\right)^{\frac{1}{2}}\right)}.$$

We should check the inequality

$$\sqrt{2\varepsilon^2 \left(\frac{1}{\Delta t} + A\Delta t\right)} \geq \frac{3}{2} (\|u^2\|_\infty^2 + \|u^1\|_\infty^2) + \frac{(3\|u^1\|_\infty^2 + 3\|u^0\|_\infty^2 + 1)^2}{2}.$$

Using the bound on  $\|u^2\|_\infty$  and  $\|u^1\|_\infty$ , we only need to verify that the choice of  $A$  in (15) ensures

$$\sqrt{2\varepsilon^2 \left(\frac{1}{\Delta t} + A\Delta t\right)} \geq C(\varepsilon^{-2} + \varepsilon^{-4}) \log\left(1 + \left(\frac{1}{\varepsilon^2 \Delta t} + \frac{A\Delta t}{\varepsilon^2} + \varepsilon^{-4}\right)^{\frac{1}{2}}\right).$$

Let  $\alpha = \frac{1}{\Delta t} + A\Delta t$ , then  $\alpha \geq 2\sqrt{A}$ . We need

$$\sqrt{2\varepsilon^2 \alpha} \geq C(\varepsilon^{-2} + \varepsilon^{-4}) \log(1 + \varepsilon^{-2} \alpha + \varepsilon^{-4}).$$

In terms of  $\varepsilon$ , we should have the following two cases.

1.  $\varepsilon^2 < 1$ , we need

$$\sqrt{\alpha} \geq C\varepsilon^{-5}(|\log \varepsilon| + |\log \alpha|).$$

or

$$\alpha \geq C\varepsilon^{-10}|\log \varepsilon|^2.$$

2.  $\varepsilon^2 \geq 1$ , we need

$$\sqrt{\alpha} \geq C\varepsilon^{-5}(|\log \alpha|),$$

or

$$\alpha \geq C.$$

From the above two cases, we can deduce the condition of  $\alpha$ ,

$$\alpha \geq C \cdot (1 + \varepsilon^{-10}|\log \varepsilon|^2). \tag{52}$$

Because  $\alpha \geq 2\sqrt{A}$ , the condition on  $A$  given in (15) ensures (52). We have  $\tilde{E}(u^2) \leq \tilde{E}(u^1)$ .

Next, we will check the induction step to prove the inequality  $\tilde{E}(u^{n+1}) \leq \tilde{E}(u^n)$ . Assume the induction hypothesis holds for all  $1 \leq \kappa \leq n, n \geq 1$ . Then for  $n + 1 (n \geq 2)$ , we only need to check the condition (34), i.e.

$$\sqrt{2\varepsilon^2 \left( \frac{1}{\Delta t} + A\Delta t \right)} \geq \frac{3}{2}(\|u^{n+1}\|_\infty^2 + \|u^n\|_\infty^2) + \frac{(3\|u^n\|_\infty^2 + 3\|u^{n-1}\|_\infty^2 + 1)^2}{2}. \tag{53}$$

By the  $L^\infty$  estimation (50) on  $u^{n+1}, u^n$  and  $u^{n-1}$ ,

$$\begin{aligned} \sqrt{2\varepsilon^2 \left( \frac{1}{\Delta t} + A\Delta t \right)} &\geq C(\varepsilon^{-2} + \varepsilon^{-4}) \log \left( 1 + \frac{1}{\varepsilon^2 \Delta t} + \frac{A\Delta t}{\varepsilon^2} + \varepsilon^{-4} \right) \\ &\quad + C(\varepsilon^{-4} + \varepsilon^{-8}) \log \left( 1 + \frac{1}{\varepsilon^2 \Delta t} + \frac{A\Delta t}{\varepsilon^2} + \varepsilon^{-4} \right)^2. \end{aligned}$$

Using the same analysis as the case  $n = 1$ , we can show that the condition on  $A$  given in (15) ensures (53). We have now completed the proof of Theorem 1.

## 5 Numerical Results

In this section, we present some numerical results for the Cahn–Hilliard equation obtained by using the IMEX LDG method, then we verify the orders of accuracy and the energy stability. In Sect. 5.1, we consider the Cahn–Hilliard equation in one spatial dimension, and test the accuracy using an explicitly given exact solution. In Sect. 5.2, the Cahn–Hilliard equation in two spatial dimension is discussed.

### 5.1 Numerical Results for the Cahn–Hilliard Equation in 1D

In this subsection we discuss the numerical results for the Cahn–Hilliard equation in 1D because there are many benchmark examples and results for this case.

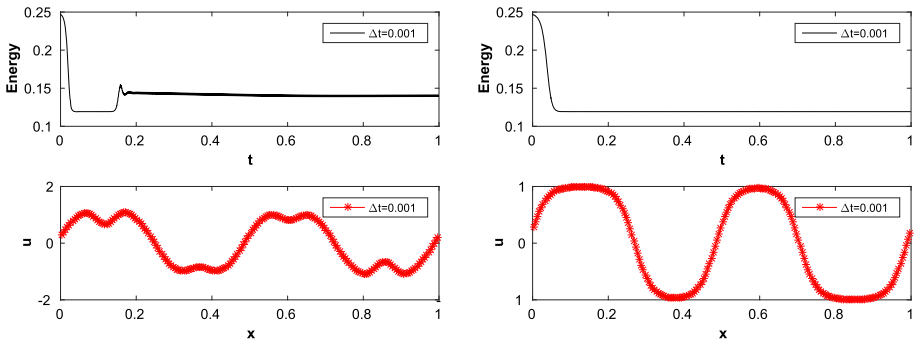


**Fig. 1** The comparison of the numerical solutions (*bottom*) and energy curves (*top*) obtained by using the LDG method with  $A = 0$  (*left*) and  $A = 10^5$  (*right*) for  $\varepsilon^2 = 0.001$

*Example 5.1* We consider

$$\begin{aligned} u_t &= (f(u) - \varepsilon^2 u_{xx})_{xx}, & (x, t) \in (0, 1] \times (0, T], \\ u(x, 0) &= u_0(x), \end{aligned} \tag{54}$$

with periodic boundary condition. The initial condition is given by

$$u_0(x) = 0.1 \sin(2\pi x) + 0.01 \cos(4\pi x) + 0.06 \sin(4\pi x) + 0.02 \cos(10\pi x). \tag{55}$$

For the spatial discretization, we use  $P^1$  and  $P^2$  elements of the LDG method to approximate (54). The dependency of the numerical solution and the energy stability on the parameter  $A$  is demonstrated in Table 1, where “NaN” denotes “not a number”. The result in the table are obtained with  $P^1$  and  $P^2$ . They have the same result, so we only list one table. From this table, we can see that the choice of the parameter  $A$  is important for the stability, which is consistent with our earlier theoretical analysis. We can also see that the size of  $A$  to ensure stability is not as pessimistic as shown in (15) from the analysis. The comparison of the numerical solutions and energy curves obtained by using the IMEX LDG method with different  $A$  is given in Fig. 1. We can see that the energy could increase and the numerical solution becomes strange when  $A = 0$ , and the energy is non-increasing and the solution looks nice when  $A = 10^5$ .

*Example 5.2* Accuracy test for the Cahn–Hilliard equation.

We consider the Cahn–Hilliard equation (54) with  $\varepsilon^2 = 1$  in the domain  $x \in [0, 2\pi]$  and with periodic boundary condition. We test our method taking the exact solution

$$u(x, t) = e^{-t} \sin x \tag{56}$$

for the Eq. (54) with a source term, which is a given function so that (56) is an exact solution. We take  $T = 1$ ,  $A = 10$  and list the  $L^2$  errors and numerical orders of accuracy with  $\Delta t = 10^{-5}$  for the second-order and third-order LDG methods in Tables 2 and 3 respectively. It is clearly observed that the IMEX LDG methods give the desired spatial order of accuracy.

Furthermore, we test accuracy for the Cahn–Hilliard equation with a smaller  $\varepsilon^2 = 0.1$  and a larger  $A = 100$  again at  $T = 1$ . This time, we aim at verifying the second order time accuracy, hence we choose  $\Delta t = h$  for the second order case and  $\Delta t = h^{3/2}$  for the third order case, to match the orders of accuracy in space and in time. The results, given in Table 4, again demonstrate the designed order of accuracy.

**Table 1** The relationship of  $A$  and the energy stability with  $\varepsilon^2 = 0.001$

$\Delta t$	$A = 0$	$A = 10^5$	$A = 5 * 10^5$
$\Delta t = 0.01$	NaN	Energy not decreasing	Energy decreasing
$\Delta t = 0.001$	Energy not decreasing	Energy decreasing	Solution is stable

**Table 2** Example 5.2: Errors and numerical order of accuracy in space for the  $P^1$ -element

$N$	$\ u - u_h\ $	Order of accuracy
16	1.21e-02	–
32	3.00e-03	2.02
64	7.43e-04	2.00
128	1.91e-04	1.96

**Table 3** Example 5.2: Errors and numerical order of accuracy in space for the  $P^2$ -element

$N$	$\ u - u_h\ $	Order of accuracy
16	6.77e-04	–
32	8.48e-05	3.00
64	1.06e-05	3.00
128	1.45e-06	2.88

**Table 4** Example 5.2: Accuracy test for the Cahn–Hilliard equation with  $\varepsilon^2 = 0.1$  at time  $T = 1$

	$N$	$\ u - u_h\ $	Order of accuracy
$P^1$	16	3.71e-01	–
$\Delta t = h$	32	1.38e-01	1.43
$A=100$	64	4.19e-02	1.72
	128	1.18e-02	1.83
$P^2$	16	5.98e-01	–
$\Delta t = h^{3/2}$	32	4.28e-01	0.48
$A=100$	64	5.64e-02	2.92
	128	6.00e-03	3.22

### 5.2 Numerical Results for the Cahn–Hilliard Equation in 2D

Now, let us turn our attention to the 2D problem.

*Example 5.3* We consider

$$\frac{\partial u}{\partial t} + \Delta(u - u^3 + \varepsilon^2 \Delta u) = 0, \tag{57}$$

and the initial condition is

$$u_0(x, y) = 0.05 \sin 2\pi x \sin 2\pi y,$$

The parameter  $\varepsilon^2$  is again taken as 0.001.  $\Omega = [0, 1] \times [0, 1]$ .

**Table 5** The relationship of  $A$  and the energy stability with  $\varepsilon^2 = 0.001$  in 2D

$\Delta t$	$A = 0$	$A = 5 * 10^5$	$A = 10^6$
$\Delta t = 0.01$	NaN	Energy not decreasing	Energy decreasing
$\Delta t = 0.001$	NaN	Energy decreasing	Solution is stable

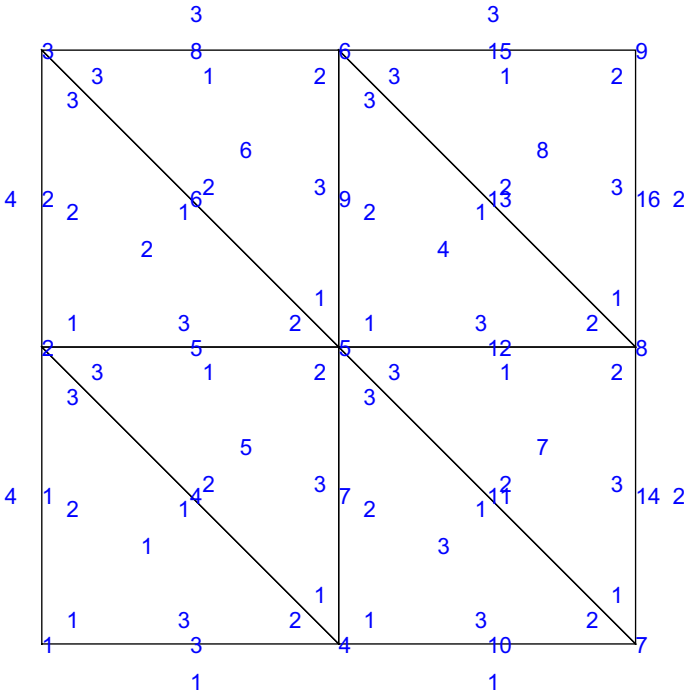


**Fig. 2** The initial triangular mesh

From Table 5, we can observe the same results as in 1D, which indicates that the parameter  $A$  plays an essential role in the stability property, and also the size of  $A$  to ensure stability is not as pessimistic as shown in (15) from the analysis.

Similarly, we verify the numerical order of convergence. A suitable source term is chosen such that

$$u(x, y, t) = 0.05e^t \sin 2\pi x \sin 2\pi y$$

is the exact solution. The physical domain is partitioned with general triangular meshes. In our experiments, the initial mesh is in Fig. 2, and in each refinement, every triangle is subdivided to four children triangles by joining the mid-points of the edges of it, see Fig. 3. Firstly, we compute with polynomial degree 1 or 2 on 32 triangles, then we refine the meshes to compute on 2048 triangles.

We take  $T = 1$ ,  $A = 100$  and list the  $L^2$  errors and the numerical orders of accuracy with  $\varepsilon^2 = 0.1$  in Table 6. The tables show that the errors decrease as the mesh resolution becomes fine, and we can clearly observe optimal orders of spatial accuracy and second-order time accuracy for the 2D Cahn–Hilliard equation on triangular meshes.

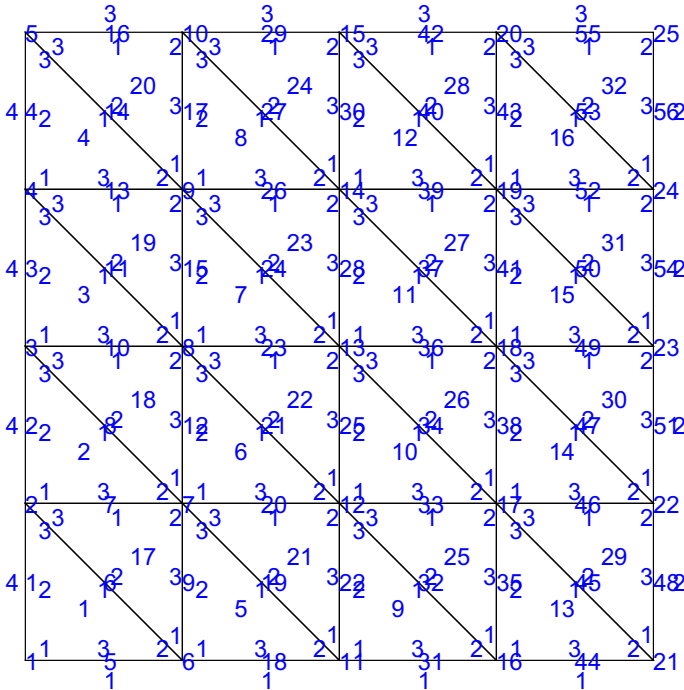


**Fig. 3** The refinement of the triangular mesh

**Table 6** Example 5.3: Accuracy test for Cahn–Hilliard equation with  $\varepsilon^2 = 0.1$  at time  $T = 1$

	h	$\ u - u_h\ $	Order of accuracy
$P^1$	1/4	1.22e-02	–
$\Delta t = h$	1/8	5.60e-03	1.12
$A=100$	1/16	1.70e-03	1.72
	1/32	4.44e-04	1.94
$P^2$	1/4	7.60e-03	–
$\Delta t = h^{3/2}$	1/8	1.20e-03	2.66
$A=100$	1/16	1.29e-04	3.21
	1/32	2.38e-05	2.44

### 6 Conclusion

In this paper, we have developed second-order implicit–explicit local discontinuous Galerkin (LDG) method for the Cahn–Hilliard equation. Unconditional energy stability independent of the time step  $\Delta t$  is proved, when the stabilization parameter  $A$  is taken to be sufficiently large but depending only on the initial data and the coefficient  $\varepsilon^2$ . This method can thus achieve substantial improvement in efficiency by using larger time steps. Using the LDG method, we have computed the Cahn–Hilliard equation in 1D and 2D. The numerical results have been presented to demonstrate the stability and approximation accuracy for the IMEX LDG method. One drawback of this method is that the stabilization parameter  $A$  has to be

chosen sufficiently large in order to ensure unconditional stability. This may adversely affect the accuracy of the scheme, especially for small  $\varepsilon$  (of course, when  $\varepsilon$  is small, the phase transition tends to be sharper and hence the accuracy deteriorates in the rapid transition region anyway). It would be interesting to look for methods which do not rely on such large stabilization parameters, can be implicit only for the linear terms as the method in this paper, and can still have unconditional energy stability.

**Acknowledgements** We would like to thank the referees for their constructive comments and suggestions which have led to an improvement of the paper.

### Appendix A: The Proof of Proposition 1

Due to the linearity and finite dimensionality of the problem, it is enough to show that the only solution to (19) and (20) with  $u = 0$  is  $v_h = 0$ .

$$\begin{aligned} (\sigma_h, \tau)_K + (v_h, \nabla \cdot \tau)_K - \langle \hat{v}_h, \tau \cdot \mathbf{n} \rangle_{\partial K} &= 0, \\ (\sigma_h, \nabla \eta)_K - \langle \hat{\sigma}_h \cdot \mathbf{n}, \eta \rangle_{\partial K} &= 0. \end{aligned}$$

Taking  $\tau = \sigma_h$  and  $\eta = v_h$ ,

$$\begin{aligned} (\sigma_h, \sigma_h)_K + (v_h, \nabla \cdot \sigma_h)_K - \langle \hat{v}_h, \sigma_h \cdot \mathbf{n} \rangle_{\partial K} &= 0, \\ (\sigma_h, \nabla v_h)_K - \langle \hat{\sigma}_h \cdot \mathbf{n}, v_h \rangle_{\partial K} &= 0. \end{aligned}$$

Applying integration by parts, and adding the two equations, we get

$$H_{\partial K}(v_h, \sigma_h)_K = (\sigma_h, \sigma_h)_K.$$

Summing over  $K$ , we can obtain

$$\sum_K (\sigma_h, \sigma_h)_K = 0$$

which implies  $\sigma_h = 0$ . Using the relationship (21), we have  $\nabla v_h = 0$  on every  $K$  and  $[v_h] = 0$ , since  $\mu > 0$ . Then  $v_h|_K = C$ . Because of  $[v_h] = 0$ ,  $v_h = C$ . However

$$\int_{\Omega} v_h dx = C \cdot |\Omega| = 0,$$

which implies  $v_h = 0$ . Thus we have completed the proof.

### Appendix B: The Proof of Lemma 3

Using the LDG discrete “inverse Laplacian” and taking  $\tau = \sigma_h^{n+1}$  and  $\eta = v_h^{n+1}$  in (22),

$$\begin{aligned} (u^{n+1} - u^n, v_h^{n+1})_K - (\sigma_h^{n+1}, \nabla v_h^{n+1})_K + \langle \hat{\sigma}_h^{n+1} \cdot \mathbf{n}, v_h^{n+1} \rangle_{\partial K} &= 0, \\ (\sigma_h^{n+1}, \sigma_h^{n+1})_K + (v_h^{n+1}, \nabla \cdot \sigma_h^{n+1})_K - \langle \hat{v}_h^{n+1}, \sigma_h^{n+1} \cdot \mathbf{n} \rangle_{\partial K} &= 0. \end{aligned}$$

Then

$$(u^{n+1} - u^n, v_h^{n+1})_K + H_{\partial K}(v_h^{n+1}, \sigma_h^{n+1})_K = (\sigma_h^{n+1}, \sigma_h^{n+1})_K.$$

Summing over  $K$  and using the Lemma 1, we can obtain the result (24).

Note that  $\delta^2 u^{n+1} = u^{n+1} - 2u^n + u^{n-1}$ , clearly

$$\begin{cases} (\delta^2 u^{n+1}, \eta)_K = (\sigma_h^{n+1} - \sigma_h^n, \nabla \eta)_K - \langle \hat{\sigma}_h^{n+1} - \hat{\sigma}_h^n \rangle \cdot \mathbf{n}, \eta >_{\partial K}, \\ (\sigma_h^{n+1}, \tau)_K = -(v_h^{n+1}, \nabla \cdot \tau)_K + \langle \hat{v}_h^{n+1}, \tau \cdot \mathbf{n} \rangle_{\partial K}. \end{cases}$$

Similarly, taking  $\eta = v_h^{n+1}$  and  $\tau = \sigma_h^{n+1} - \sigma_h^n$ ,

$$\begin{aligned} (\delta^2 u^{n+1}, v_h^{n+1})_K - (\sigma_h^{n+1} - \sigma_h^n, \nabla v_h^{n+1})_K + \langle \hat{\sigma}_h^{n+1} - \hat{\sigma}_h^n \rangle \cdot \mathbf{n}, v_h^{n+1} >_{\partial K} &= 0, \\ (\sigma_h^{n+1}, \sigma_h^{n+1} - \sigma_h^n)_K + (v_h^{n+1}, \nabla \cdot (\sigma_h^{n+1} - \sigma_h^n))_K - \langle \hat{v}_h^{n+1}, (\sigma_h^{n+1} - \sigma_h^n) \cdot \mathbf{n} \rangle_{\partial K} &= 0. \end{aligned}$$

So that

$$\begin{aligned} (\delta^2 u^{n+1}, v_h^{n+1})_K + H_{\partial K} (v_h^{n+1}, \sigma_h^{n+1} - \sigma_h^n) \\ = (\sigma_h^{n+1}, \sigma_h^{n+1} - \sigma_h^n)_K. \end{aligned}$$

Summing over  $K$  and using the Lemma 1, we can obtain the result (25). This completes the proof.

### Appendix C: The Proof of the Lemma 7

Taking  $\rho = \varepsilon^2 u^1$ ,  $\mathbf{q} = -\varepsilon^2 \mathbf{w}^1$ ,  $\phi = p^1 - r^0$ ,  $\psi = \varepsilon^2 (\mathbf{s}_1^0 - \mathbf{s}_2^1)$  in Eqs. (51), and using the same analysis as the Lemma 6, we have

$$\frac{\varepsilon^2}{t_1} (u^1 - u^0, u^1) + (p^1, p^1 - r^0) = 0.$$

Summing up over  $K$ ,

$$\frac{\varepsilon^2}{t_1} \cdot (\|u^1\|^2 - \|u^0\|^2) + \|p^1\|^2 \leq \frac{1}{2} (\|p^1\|^2 + \|r^0\|^2),$$

So we have the result

$$\|u^1\|^2 \leq \|u^0\|^2 + \frac{t_1}{\varepsilon^2} \|f(u^0)\|^2,$$

and

$$\|p^1\|^2 \leq \frac{\varepsilon^2}{t_1} \|u^0\|^2 + \|f(u^0)\|^2,$$

By the definition of the discrete Laplacian operator,

$$(p^1, \phi) = -\varepsilon^2 (-\Delta_h u^1, \phi),$$

Then Taking  $\phi = -\Delta_h u^1$ , we obtain

$$\|\Delta_h u^1\|^2 \leq \frac{1}{\varepsilon^2 t_1} \|u^0\|^2 + \frac{1}{\varepsilon^4} \|f(u^0)\|^2,$$

Next, taking  $\rho = v_h^1 = (-\Delta)^{-1} (u^1 - u^0)$ ,  $\mathbf{q} = \sigma_h^1$ ,  $\phi = u^1 - u^0$ ,  $\xi = u^1 - u^0$  in Eqs. (51), and

$$(\mathbf{w}^1 - \mathbf{w}^0, \mathbf{w}^1)_K = (\nabla (u^1 - u^0), \mathbf{w}^1)_K + H_{\partial K} (u^1 - u^0, \mathbf{w}^1) - \langle \hat{\mathbf{w}}^1 \cdot \mathbf{n}, u^1 - u^0 \rangle_{\partial K},$$



using the same argument as Eqs. (36)–(48), then

$$\left(\frac{u^1 - u^0}{t_1}, v_h^1\right)_K + \varepsilon^2(\mathbf{w}^1 - \mathbf{w}^0, \mathbf{w}^1)_K + (f(u^0), u^1 - u^0)_K - \varepsilon^2 H_{\partial K}(u^1 - u^0, \mathbf{w}^1) = 0.$$

Using Lemmas 1, 3, and summing on  $K$ ,

$$\begin{aligned} & \frac{1}{t_1} \|\sigma_h^1\|^2 + \frac{\varepsilon^2}{2} \|\mathbf{w}^1\|^2 + \sum_K (F(u^1), 1) \\ & \leq E(u^0) + |f'(u^0)| \cdot \|u^1 - u^0\|^2 \\ & \leq C(E(u^0), \|u^0\|_{H^4}). \end{aligned}$$

So that

$$\|\mathbf{w}^1\|^2 \leq C(E(u^0), \|u^0\|_{H^4}) \frac{1}{\varepsilon^2},$$

Finally, by the Lemma 4,

$$\|u^1\|_\infty \leq C\sqrt{1 + \varepsilon^{-1}} \cdot \sqrt{\log\left(1 + \left(\frac{1}{\varepsilon^2 t_1} + \varepsilon^{-4}\right)^{\frac{1}{2}}\right)}.$$

## References

1. Arnold, D.N., Brezzi, F., Cockburn, B., Marini, L.D.: Unified analysis of discontinuous Galerkin methods for elliptic problems. *SIAM J. Numer. Anal.* **39**, 1749–1779 (2002)
2. Ascher, U.M., Ruuth, J., Spiteri, R.J.: Implicit–explicit Runge–Kutta method for time dependent partial differential equations. *Appl. Numer. Math.* **25**, 151–167 (1997)
3. Ascher, U.M., Ruuth, J., Wetton, T.R.: Implicit–explicit method for time dependent partial differential equations. *SIAM. J. Numer. Anal.* **32**, 797–823 (1995)
4. Bassi, F., Rebay, S.: A high-order accurate discontinuous finite element method for the numerical solution of the compressible Navier–Stokes equations. *J. Comput. Phys.* **131**, 267–279 (1997)
5. Brezis, H., Gallout, T.: Nonlinear Schrodinger evolution equations. *Nonlinear Anal. Theory Meth. Appl.* **4**, 677–681 (1980)
6. Cahn, J.W., Hilliard, J.E.: Free energy of a nonuniform system. I. Interfacial free energy. *J. Chem. Phys.* **28**, 258–267 (1958)
7. Choo, S.M., Chung, S.K., Kim, K.I.: Conservative nonlinear difference scheme for the Cahn–Hilliard equation-II. *Comput. Math. Appl.* **39**, 229–243 (2000)
8. Cockburn, B., Shu, C.-W.: The local discontinuous Galerkin method for time-dependent convection–diffusion systems. *SIAM J. Numer. Anal.* **35**, 2440–2463 (1998)
9. Furihata, D.: A stable and conservative finite difference scheme for the Cahn–Hilliard equation. *Numer. Math.* **87**, 675–699 (2001)
10. Dong, B., Shu, C.-W.: Analysis of a local discontinuous Galerkin method for linear time-dependent fourth-order problems. *SIAM J. Numer. Anal.* **47**, 3240–3268 (2009)
11. Elliott, C.M., French, D.A.: A nonconforming finite element method for the two-dimensional Cahn–Hilliard equations. *SIAM J. Numer. Anal.* **26**, 884–903 (1989)
12. Elliott, C.M., Larsson, S.: Error estimates with smooth and nonsmooth data for a finite element method for the Cahn–Hilliard equation. *Math. Comput.* **58**, 603–630 (1992)
13. Elliott, C.M., Stinner, B.: Computation of two-phase biomembranes with phase dependent material parameters using surface finite elements. *Commun. Comput. Phys.* **13**, 325–360 (2013)
14. Eyre, D.J.: An unconditionally stable one-step scheme for gradient systems. Available at <http://www.math.utah.edu/~eyre/research/methods/stable.ps> (1998)
15. Eyre, D.J.: Unconditionally gradient stable time marching the Cahn–Hilliard equation. *Mater. Res. Soc. Sympos. Proc.* **529**, 39–46 (1998)

16. Feng, X.L., Song, H., Tang, Tao, Yang, J.: Nonlinear stability of the implicit–explicit methods for the Allen–Cahn equation. *Inverse Probl Imaging* **7**, 679–695 (2013)
17. Guo, R., Xu, Y.: Efficient solvers of DG discretization for the Cahn–Hilliard equations. *SIAM J. Sci. Comput.* **58**, 380–408 (2014)
18. He, Y.N., Liu, Y.X., Tang, T.: On large time-stepping methods for the Cahn–Hilliard equation. *Appl. Numer. Math.* **57**, 616–628 (2007)
19. Li, D., Qiao, Z.: On second order semi-implicit fourier spectral methods for 2D Cahn–Hilliard equations. *J. Sci. Comput.* **70**, 301–341 (2017)
20. Qiao, Z., Zhang, Z., Tang, T.: An adaptive time-stepping strategy for the molecular beam epitaxy models. *SIAM J. Sci. Comput.* **33**, 1395–1414 (2011)
21. Shen, J., Yang, X.: Numerical approximations of Allen–Cahn and Cahn–Hilliard equations. *Discrete Contin. Dyn. Syst. A* **28**, 1669–1691 (2010)
22. Song, H.: Energy stable and large time-stepping methods for the Cahn–Hilliard equation. *Inter. J. Comput. Math.* **92**, 2091–2108 (2015)
23. Sun, Z.Z.: A second-order accurate linearized difference scheme for the two-dimensional Cahn–Hilliard equation. *Math. Comput.* **64**, 1463–1471 (1995)
24. Xu, C., Tang, T.: Stability analysis of large time-stepping methods for epitaxial growth models. *SIAM J. Num. Anal.* **44**, 1759–1779 (2006)
25. Xu, Y., Shu, C.-W.: Local discontinuous Galerkin methods for high-order time-dependent partial differential equations. *Commun. Comput. Phys.* **7**, 1–46 (2016)
26. Wang, H., Wang, S., Zhang, Q., Shu, C.-W.: Local discontinuous Galerkin methods with implicit–explicit time-marching for multi-dimensional convection–diffusion problems. *ESAIM: Math. Model. Numer. Anal.* **50**, 1083–1105 (2016)
27. Zhang, Z., Qiao, Z.: An adaptive time-stepping strategy for the Cahn–Hilliard equation. *Commun. Comput. Phys.* **11**, 1261–1278 (2012)